

Atmospheric Chemistry of 1,2-Dichloroethane: UV Spectra of CH₂ClCHCl and CH₂ClCHClO₂ Radicals, Kinetics of the Reactions of CH₂ClCHCl Radicals with O₂ and CH₂ClCHClO₂ Radicals with NO and NO₂, and Fate of the Alkoxy Radical CH₂ClCHClO

Timothy J. Wallington*

Ford Research Laboratory, SRL-3083, Ford Motor Company, P.O. Box 2053, Dearborn, Michigan 48121-2053

Merete Bilde, Trine E. Møgelberg, and Jens Sehested

Section for Chemical Reactivity, Environmental Science and Technology Department, Risø National Laboratory, DK-4000 Roskilde, Denmark

Ole J. Nielsen*

Ford Motor Company, Ford Forschungszentrum Aachen, Dennewartstrasse 25, D-52068 Aachen, Germany

Received: July 27, 1995; In Final Form: January 24, 1996[⊗]

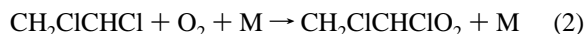
A pulse radiolysis technique was used to measure the UV absorption spectra of CH₂ClCHCl and CH₂ClCHClO₂ radicals over the range 230–300 nm. At 250 nm, $\sigma(\text{CH}_2\text{ClCHCl}) = (1.7 \pm 0.2) \times 10^{-18}$ and $\sigma(\text{CH}_2\text{ClCHClO}_2) = (3.5 \pm 0.5) \times 10^{-18}$ cm² molecule⁻¹. The observed self-reaction rate constant for CH₂ClCHCl radicals, defined as $-d[\text{CH}_2\text{ClCHCl}]/dt = 2k_4[\text{CH}_2\text{ClCHCl}]^2$ was $k_4 = (2.0 \pm 0.3) \times 10^{-11}$ cm³ molecule⁻¹ s⁻¹. The rate constant for reaction of CH₂ClCHCl radicals with O₂ in one bar of SF₆ diluent was $(2.4 \pm 0.3) \times 10^{-12}$ cm³ molecule⁻¹ s⁻¹. The rate constants for the reactions of CH₂ClCHClO₂ radicals with NO and NO₂ were $k_5 \geq 9 \times 10^{-12}$ and $k_6 = (9.8 \pm 0.6) \times 10^{-12}$ cm³ molecule⁻¹ s⁻¹, respectively. The rate constant for the reaction of F atoms with CH₂ClCH₂Cl was $k_3 = (2.6 \pm 0.2) \times 10^{-11}$ cm³ molecule⁻¹ s⁻¹. The reaction of CH₂ClCHClO₂ radicals with NO produced NO₂ and, by implication, CH₂ClCHClO radicals. A FTIR spectroscopic technique showed that CH₂ClCHClO radicals undergo both reaction with O₂ and decomposition via intramolecular 3-center HCl elimination. In 700 Torr of air at 296 K the rate constant ratio $k_{\text{O}_2}/k_{\text{decomp}} = (2.3 \pm 0.2) \times 10^{-20}$ cm³ molecule⁻¹. A lower limit of 4×10^5 s⁻¹ was deduced for the rate of intramolecular 3-center HCl elimination from CH₂ClCHClO radicals at 296 K in 1 bar of SF₆ diluent. As part of this work a relative rate technique was used to measure rate constants of $(1.3 \pm 0.2) \times 10^{-12}$ and $(6.4 \pm 1.4) \times 10^{-14}$ cm³ molecule⁻¹ s⁻¹ for the reactions of Cl atoms with CH₂ClCH₂Cl and CH₂ClC(O)Cl, respectively. All experiments were performed at 296 K. Results are discussed in the context of the atmospheric chemistry of 1,2-dichloroethane.

1. Introduction

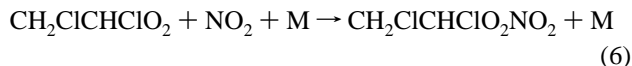
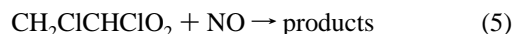
Assessment of the environmental impact of organic compounds released into the atmosphere requires a detailed understanding of their atmospheric degradation. Alkoxy radicals are key intermediates in the atmospheric oxidation of all organic compounds. Until 1993 it was believed that the atmospheric fate of alkoxy radicals was either reaction with O₂, isomerization, or decomposition (via C–C bond scission or halogen atom elimination). Recent experimental studies at Ford Motor Company have demonstrated the existence of another atmospheric fate for α -monochloroalkoxy radicals; namely intramolecular elimination of HCl.^{1–4} At the present time there are significant uncertainties in our understanding of the atmospheric chemistry of alkoxy radicals.

To provide insight into the atmospheric chemistry of halogenated alkoxy radicals and hence improve the technical basis for predictions of the environmental impact of halogenated organics we have conducted a study of the atmospheric chemistry of 1,2-dichloroethane. This compound was selected for study because of its structural similarity to HFC-152 (CH₂FCH₂F) and HFC-134 (CHF₂CHF₂) which are under consideration as CFC replacements. In the troposphere 1,2-

dichloroethane (CH₂ClCH₂Cl) will react with OH radicals to produce alkyl radicals which will, in turn, react with O₂ to give peroxy radicals:



In the present work we have used pulse radiolysis to determine the UV absorption spectra of CH₂ClCHCl and CH₂ClCHClO₂ radicals, and the kinetics of reactions 2–6.



FTIR product studies were used to study the atmospheric fate of the alkoxy radical CH₂ClCHClO. The results presented herein improve our understanding of the atmospheric chemistry

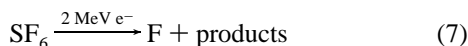
* Authors to whom correspondence may be addressed.

[⊗] Abstract published in *Advance ACS Abstracts*, March 15, 1996.

of alkoxy radicals and hence improve our ability to predict the environmental impact of the release of organic compounds.

2. Experimental Section

2.1. Pulse Radiolysis System. The pulse radiolysis transient UV absorption setup used for the present experiments has been described in detail previously and will only be dealt with briefly here.⁵ CH₂ClCHCl radicals were generated by the radiolysis of SF₆/CH₂ClCH₂Cl gas mixtures in a 1 L stainless steel reactor with a 30 ns pulse of 2 MeV electrons from a Febetron 705B field emission accelerator. SF₆ was always in great excess and was used to generate fluorine atoms:



Six sets of experiments were performed. First, the kinetics of the formation of CH₂ClCHCl was monitored using its absorption at 250 nm to provide kinetic data for the reaction of F atoms with CH₂ClCH₂Cl. Second, the rate of reaction of CH₂ClCHCl radicals with O₂ was established by following the formation of CH₂ClCHClO₂ radicals in reaction mixtures containing O₂. Third, the ultraviolet absorption spectra of CH₂ClCHCl and CH₂ClCHClO₂ radicals were determined by observing the maximum of the transient UV absorption at short times (0–2 μs) following the pulse radiolysis of SF₆/CH₂ClCH₂Cl and SF₆/CH₂ClCH₂Cl/O₂ mixtures, respectively. Fourth, using a longer time scale (5–400 μs), the decay of the absorption ascribed to CH₂ClCHCl radicals was monitored to determine the kinetics of the self-reaction (eq 4):



Fifth, the rate of NO₂ formation following the pulse radiolysis of SF₆/CH₂ClCH₂Cl/O₂/NO mixtures was used to measure *k*₅. Sixth, the rate of decay of NO₂ following the pulse radiolysis of SF₆/CH₂ClCH₂Cl/O₂/NO₂ mixtures was used to measure *k*₆.

To monitor the transient UV absorption, the output of a pulsed 150 W xenon arc lamp was multi-passed through the reaction cell using internal White type optics (80 or 120 cm path length). Reagent concentrations used were as follows: SF₆, 960–970 mbar; O₂, 0–33 mbar; CH₂ClCH₂Cl, 0–10.0 mbar; NO, 0–1.57 mbar; and NO₂ 0–1.16 mbar (1013 mbar = 760 Torr). All experiments were performed at 296 K. Ultra-high purity O₂ was supplied by L'Air Liquide, SF₆ (99.9%) was supplied by Gerling and Holz, CH₂ClCH₂Cl (>99.8%) was obtained from Aldrich, NO (>99.8%) was supplied by Messer Griesheim, and NO₂ (>98%) was supplied by Linde Technische Gase. The CH₂ClCH₂Cl sample was degassed before use by repeated freeze–pump–thaw cycling. All other reagents were used as received. No evidence for absorption by CH₂ClCH₂Cl over the 230–300 nm wavelength range was discernable in the present experiments, $\sigma(230 \text{ nm}) < 10^{-21} \text{ cm}^2 \text{ molecule}^{-1}$.

2.2. FTIR-Smog Chamber System. The FTIR system was interfaced to a 140 L Pyrex reactor. Radicals were generated by the UV irradiation of mixtures of 110–130 mTorr of CH₂ClCH₂Cl, 34–300 mTorr of Cl₂, and 15–700 Torr of O₂ in 700 Torr total pressure with N₂ diluent at 296 K using 22 blacklamps (760 Torr = 1013 mbar). The loss of reactants and the formation of products were monitored by FTIR spectroscopy, using an analyzing path length of 27 m and a resolution of 0.25 cm⁻¹. Infrared spectra were derived from 32 coadded spectra. CH₂ClCH₂Cl, CH₂ClC(O)Cl, HC(O)Cl, and CO₂ were monitored using their characteristic features over the wavenumber ranges 1200–1350, 1800–1900, 1720–1820, and 2280–2400 cm⁻¹, respectively. With the exception of HC(O)Cl, reference

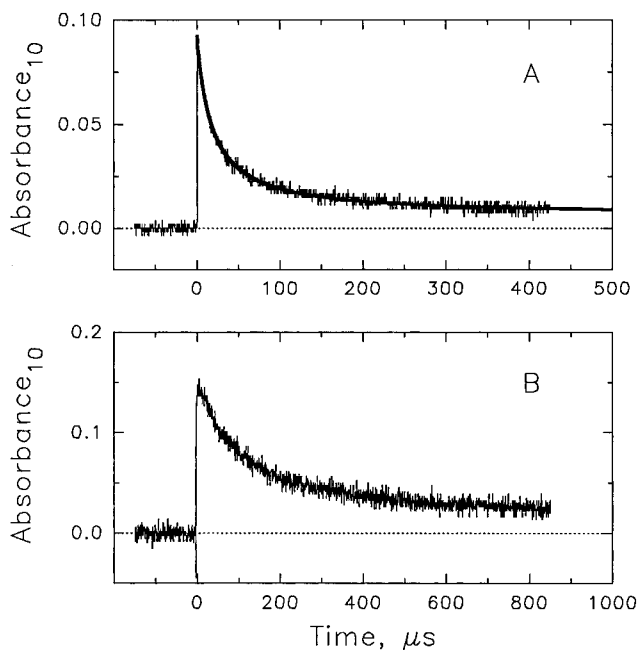
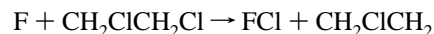


Figure 1. Transient absorbance at 250 nm following the pulsed radiolysis of a mixture of (A) 10 mbar CH₂ClCH₂Cl and 990 mbar SF₆ (radiolysis dose was 53% of maximum dose) and (B) 5 mbar CH₂ClCH₂Cl, 30 mbar O₂, and 965 mbar SF₆ (radiolysis dose was 42% of maximum dose). UV pathlength was 80 cm.

spectra were acquired and calibrated by expanding known volumes of reference materials into the reactor. The reference spectrum of HC(O)Cl obtained from the reference library at Ford Motor Company was calibrated using $\sigma(1793 \text{ cm}^{-1}) = 1.63 \times 10^{-18} \text{ cm}^2 \text{ molecule}^{-1}$.

3. Results and Discussion

3.1. Kinetics of F + CH₂ClCH₂Cl. Following the pulse radiolysis of CH₂ClCH₂Cl/SF₆ mixtures, a rapid increase in absorption in the UV at 250 nm was observed, followed by a slower decay. Figure 1A shows the transient absorption at 250 nm following the radiolysis of a mixture of 10 mbar CH₂ClCH₂Cl and 990 mbar SF₆. No absorption was observed when either 10 mbar of CH₂ClCH₂Cl or 990 mbar of SF₆ was radiolyzed separately. We assume that reaction of F atoms with CH₂ClCH₂Cl proceeds exclusively via H atom abstraction. To the best of our knowledge, the heat of formation of CH₂ClCH₂ radicals has not been reported and we are unable to calculate the thermochemistry of the chlorine abstraction channel:



However, relevant data are available to evaluate the thermodynamics of analogous reactions involving CH₃Cl, CH₂Cl₂, and C₂H₅Cl.⁷ Cl atom abstraction from CH₃Cl, CH₂Cl₂, and C₂H₅Cl is endothermic by 23–24 kcal mol⁻¹. It seems reasonable to conclude that the reaction of F atoms with CH₂ClCH₂Cl proceeds exclusively to give CH₂ClCHCl radicals. We ascribe the absorption shown in Figure 1A to the formation of CH₂ClCHCl radicals and their subsequent loss by self-reaction. The increase in absorption at short times (0–10 μs) followed pseudo-first-order kinetics. Figure 2 shows a plot of the pseudo-first-order rate constants for the appearance of absorption (filled symbols) as a function of the CH₂ClCH₂Cl concentration. The solid line in Figure 2 through the filled symbols is a linear least-squares fit which gives a slope of $k_3 = (2.6 \pm 0.2) \times 10^{-11} \text{ cm}^3 \text{ molecule}^{-1} \text{ s}^{-1}$. The positive intercept is $(3.9 \pm 1.8) \times 10^5 \text{ s}^{-1}$ and is statistically significant. To investigate the cause of

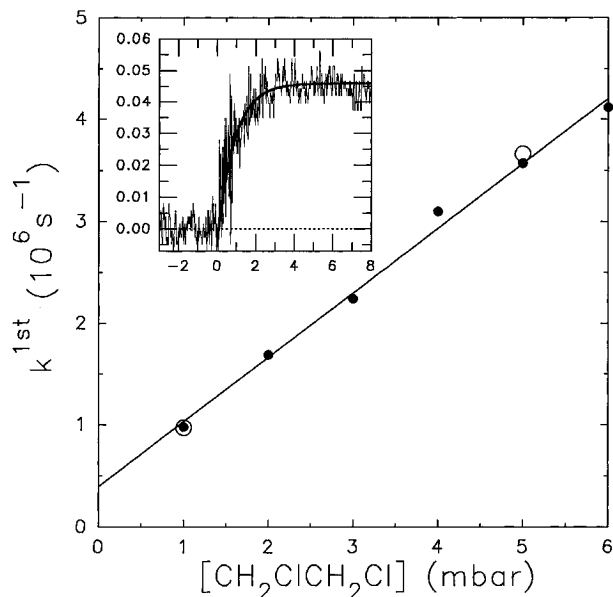


Figure 2. Pseudo-first-order rate constants for the increase in absorption at 250 nm following radiolysis of mixtures of 1–6 mbar of $\text{CH}_2\text{ClCH}_2\text{Cl}$ and 1000 mbar of SF_6 vs $[\text{CH}_2\text{ClCH}_2\text{Cl}]$. Filled symbols are observed data; open symbols are the results of simulations described in the text. The insert shows the experimental transient using a mixture of 1 mbar $\text{CH}_2\text{ClCH}_2\text{Cl}$ and 999 mbar of SF_6 , the UV pathlength was 80 cm and the radiolysis dose was 32% of maximum. The smooth curve in the insert is the first order fit.

the positive intercept, the CHEMSIMUL⁸ chemical kinetic modeling package was used to simulate the rise in absorption by CH_2ClCHCl radicals using a chemical mechanism consisting of reactions 3 and 4 with $k_3 = 2.6 \times 10^{-11} \text{ cm}^3 \text{ molecule}^{-1} \text{ s}^{-1}$ and $k_4 = 2.3 \times 10^{-11} \text{ cm}^3 \text{ molecule}^{-1} \text{ s}^{-1}$ (see subsequent section). Two data points were simulated. The simulated rise in absorption followed pseudo-first-order kinetics and a first-order kinetic expression was fit to the simulated data to give the results shown as the open circles in Figure 2. As seen from Figure 2, within the experimental uncertainties, the simulated data and experimental data are indistinguishable. We conclude that the cause of the positive intercept is the CH_2ClCHCl radical self-reaction which decreases the time taken for the absorption to react a maximum and hence increases the values of k^{1st} obtained. No correction to the value of $k_3 = 2.6 \times 10^{-11} \text{ cm}^3 \text{ molecule}^{-1} \text{ s}^{-1}$ is needed. Quoted errors throughout this paper are two standard deviations. Where appropriate, errors have been propagated using standard error analysis techniques.

3.2. Kinetics of $\text{CH}_2\text{ClCHCl} + \text{O}_2$. The kinetics of the reaction of CH_2ClCHCl radicals with O_2 were investigated by radiolysis of $\text{CH}_2\text{ClCH}_2\text{Cl}/\text{O}_2/\text{SF}_6$ mixtures with the resulting transient absorption monitored at 250 nm. As seen from Figure 1B, the transient absorption at 250 nm following radiolysis of mixtures containing O_2 was substantially larger than that observed in the absence of O_2 . This observation suggests that a given concentration of peroxy radicals derived from 1,2 dichloroethane ($\text{CH}_2\text{ClCHClO}_2$) absorbs more strongly than the same concentration of alkyl radicals (CH_2ClCHCl). Such a finding is reasonable upon the basis of the substantial database concerning the UV spectra of peroxy radicals which shows that these species absorb strongly at 250 nm.^{9,10} Kinetic data for the reaction of CH_2ClCHCl radicals with O_2 were obtained by observing the kinetics of the increase in absorption at 250 nm following the radiolysis of mixtures of 20 mbar of $\text{CH}_2\text{ClCH}_2\text{Cl}$, 6–33 mbar of O_2 , and 960 mbar of SF_6 mixtures. The lifetime of F atoms in the presence of 10 mbar of $\text{CH}_2\text{ClCH}_2\text{Cl}$ is 0.08 μs . Hence, the absorption rise was fitted from 1 μs

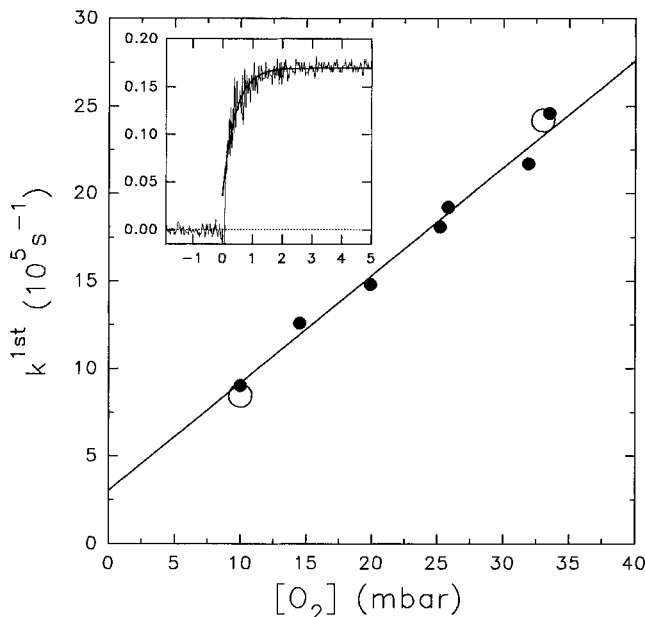


Figure 3. Pseudo-first-order rate constants for the increase in absorption at 250 nm following radiolysis of mixtures of 20 mbar of $\text{CH}_2\text{ClCH}_2\text{Cl}$, 10–33.5 mbar of O_2 , and 1000 mbar of SF_6 vs $[\text{O}_2]$. Filled symbols are observed data; open symbols are the results of simulations described in the text. The insert shows the experimental transient using a mixture of 20 mbar $\text{CH}_2\text{ClCH}_2\text{Cl}$, 25.8 mbar of O_2 , and 960 mbar of SF_6 ; the UV pathlength was 80 cm and the radiolysis dose was 53% of maximum. The smooth curve in the insert is the first order fit.

after the radiolysis pulse to allow for conversion of F atoms into CH_2ClCHCl radicals. The subsequent increase in absorption followed first-order kinetics. Figure 3 shows the observed pseudo-first-order rate constants (filled circles) as a function of O_2 concentration. A linear regression analysis of the data in Figure 3 (filled circles) gives $k_2 = (2.4 \pm 0.3) \times 10^{-12} \text{ cm}^3 \text{ molecule}^{-1} \text{ s}^{-1}$, the y axis intercept is $(3.5 \pm 1.2) \times 10^4 \text{ s}^{-1}$. To investigate the cause of the positive intercept the CHEMSIMUL⁸ chemical kinetic modeling package was used to simulate the rise in absorption by $\text{CH}_2\text{ClCHClO}_2$ radicals using a chemical mechanism consisting of reactions 2, 3, and 4 with $k_2 = 2.4 \times 10^{-12}$, $k_3 = 2.6 \times 10^{-11}$, and $k_4 = 2.3 \times 10^{-11} \text{ cm}^3 \text{ molecule}^{-1} \text{ s}^{-1}$. The $\text{CH}_2\text{ClCHClO}_2$ radical self-reaction was included in the model with $k_{\text{RO}_2+\text{RO}_2} = 3.0 \times 10^{-12} \text{ cm}^3 \text{ molecule}^{-1} \text{ s}^{-1}$ which describes the observed decay of absorption at 250 nm seen in Figure 1B. Two data points were simulated. The simulated rise in absorption followed pseudo-first-order kinetics. A first-order kinetic expression was fit to the simulated data to give the results shown as the open circles in Figure 3. As seen from Figure 3, within the experimental uncertainties, the simulated data and experimental data are indistinguishable. We conclude that the cause of the positive intercept are the self-reactions of the CH_2ClCHCl and $\text{CH}_2\text{ClCHClO}_2$ radicals which decrease the time taken for the absorption to react a maximum and hence increase the values of k^{1st} obtained. The modeling exercise shows that the slope of the data plot in Figure 3 is not influenced by secondary reactions. Hence, $k_2 = (2.4 \pm 0.3) \times 10^{-12} \text{ cm}^3 \text{ molecule}^{-1} \text{ s}^{-1}$.

3.3. Spectrum of CH_2ClCHCl Radicals. Measurement of the absolute absorption spectrum of CH_2ClCHCl radicals requires calibration of the initial F atom concentration. Additionally, experimental conditions are needed to ensure that there is 100% conversion of F atoms to CH_2ClCHCl radicals. The yield of F atoms was established by monitoring the transient absorbance at 260 nm due to methylperoxy radicals produced by radiolysis of $\text{SF}_6/\text{CH}_4/\text{O}_2$ mixtures as described previously.¹¹

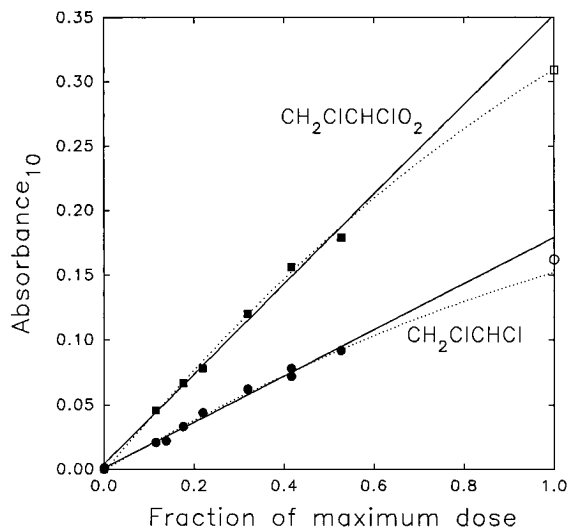
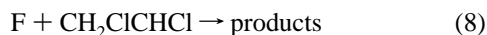


Figure 4. Maximum transient absorbance at 250 nm following the pulsed radiolysis of mixtures of 10 mbar $\text{CH}_2\text{ClCH}_2\text{Cl}$ and 990 mbar SF_6 (circles) or 5 mbar $\text{CH}_2\text{ClCH}_2\text{Cl}$, 30 bar of O_2 , and 965 mbar SF_6 (squares) as functions of the radiolysis dose. The UV pathlength was 80 cm. The solid lines are linear regressions of the low-dose data (filled symbols). The dotted lines are second-order regressions to the entire data set to aid visual inspection.

Using a value of $3.18 \times 10^{-18} \text{ cm}^2 \text{ molecule}^{-1}$ for $\sigma(\text{CH}_3\text{O}_2)$ at 260 nm,⁹ the yield of F atoms at 1000 mbar of SF_6 was determined to be $(3.0 \pm 0.3) \times 10^{15} \text{ molecules cm}^{-3}$ at full irradiation dose. The quoted error on the F atom calibration includes both statistical (± 2 standard deviations) and potential systematic errors associated with the 10% uncertainty in $\sigma(\text{CH}_3\text{O}_2)$. In the following, errors are propagated using conventional error analysis methods and are shown as ± 2 standard deviations.

To work under conditions where the F atoms are converted stoichiometrically into CH_2ClCHCl radicals, it is necessary to consider potential interfering secondary chemistry. A complication could be reaction 8.



To check for complications caused by reaction 8, experiments were performed using $[\text{CH}_2\text{ClCH}_2\text{Cl}] = 10 \text{ mbar}$ and $[\text{SF}_6] = 990 \text{ mbar}$ in which the maximum transient absorption at 250 nm was measured as a function of the radiolysis dose. Figure 4 shows the observed maximum transient absorption (optical path length = 80 cm) ascribed to CH_2ClCHCl radicals as a function of the dose. As shown in Figure 4, the maximum absorption observed in experiments using maximum dose was slightly less than that expected on the basis of a linear extrapolation of the data obtained at lower doses. This observation suggests that reaction 8 is important in experiments using the maximum initial F atom concentration.

The solid line drawn through the CH_2ClCHCl data in Figure 4 is a linear least-squares fit to the low-dose data and has a slope of 0.178 ± 0.011 . Combining this data with the calibrated yield of F atoms of $(3.0 \pm 0.3) \times 10^{15} \text{ molecules cm}^{-3}$ (full dose and $[\text{SF}_6] = 1000 \text{ mbar}$) gives $\sigma(\text{CH}_2\text{ClCHCl})$ at 250 nm = $(1.71 \pm 0.20) \times 10^{-18} \text{ cm}^2 \text{ molecule}^{-1}$. Quoted errors reflect uncertainties in both the F atom calibration and the slope of the line drawn in Figure 4. To map out the absorption spectrum of CH_2ClCHCl radicals, experiments were performed to measure the initial absorption between 230 and 280 nm following the pulsed irradiation of mixtures of 10 mbar of $\text{CH}_2\text{ClCH}_2\text{Cl}$ and 990 mbar of SF_6 . Initial absorptions were then scaled to that

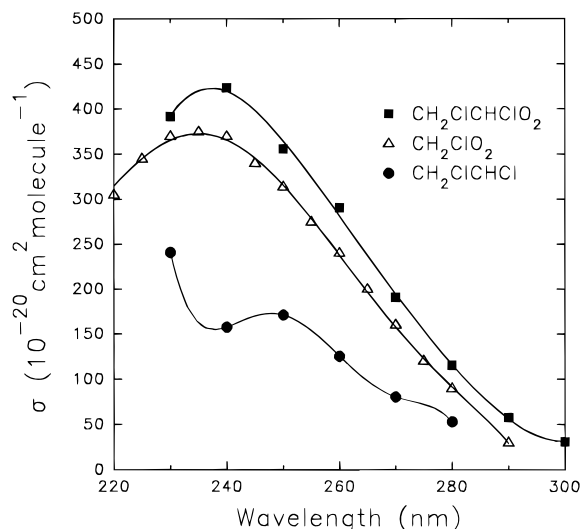


Figure 5. UV absorption spectra of radical species: CH_2ClCHCl (●), this work; $\text{CH}_2\text{ClCHClO}_2$ (■), this work; CH_2ClO_2 (▲).¹³

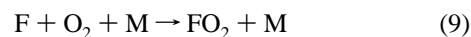
TABLE 1

wavelength (nm)	$\sigma(\text{CH}_2\text{ClCHCl})$ ($10^{-20} \text{ cm}^2 \text{ molecule}^{-1}$)	$\sigma(\text{CH}_2\text{ClCHClO}_2)$ ($10^{-20} \text{ cm}^2 \text{ molecule}^{-1}$)
230	240	390
240	160	420
250	170	350
260	130	290
270	80	190
280	53	120
290	—	57
300	—	31

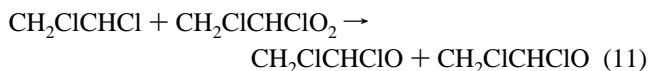
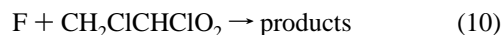
at 250 nm and converted into absolute absorption cross sections. Values obtained are given in Table 1 and plotted in Figure 5.

3.4. Spectrum of $\text{CH}_2\text{ClCHClO}_2$ Radicals. Following the pulsed radiolysis of mixtures of 5 mbar of $\text{CH}_2\text{ClCH}_2\text{Cl}$, 30 mbar of O_2 , and 965 mbar of SF_6 a rapid increase, complete within 5 μs , in UV absorbance in the region 230–300 nm was observed, followed by a slower decay. An example is shown in Figure 1B. We ascribe the UV absorbance resulting from radiolysis of $\text{SF}_6/\text{CH}_2\text{ClCH}_2\text{Cl}/\text{O}_2$ mixtures to $\text{CH}_2\text{ClCHClO}_2$ radicals.

To work under conditions where the F atoms are converted stoichiometrically into $\text{CH}_2\text{ClCHClO}_2$ radicals, it is necessary to consider potential interfering secondary chemistry. Potential complications include: (i) Loss of F atoms by reaction with molecular oxygen



and (ii) unwanted radical–radical reactions such as reactions 4, 8, 10, and 11.



Using rate constants for reactions 3 and 9, $k_3 = (2.4 \pm 0.2) \times 10^{-11}$ (this work) and $k_9 = (1.9 \pm 0.3) \times 10^{-13} \text{ cm}^3 \text{ molecule}^{-1} \text{ s}^{-1}$,¹² we calculate that 4.5% of the F atoms are converted into FO_2 radicals and 95.5% into $\text{CH}_2\text{ClCHClO}_2$ radicals. Decomposition of FO_2 radicals back to F atoms and O_2 is of no importance over the $< 5 \mu\text{s}$ taken for the absorption to reach its maximum. Corrections for the presence of 4.5% of FO_2 radicals were calculated using the expression $\sigma(\text{CH}_2\text{ClCHClO}_2) =$

$[\sigma(\text{observed}) - 0.045 \times \sigma(\text{FO}_2)]/0.955$. Values of $\sigma(\text{FO}_2)$ are taken from the literature.¹² Corrections to account for FO_2 absorption were minor (1–5%).

There are no literature data concerning the kinetics of reactions 8, 10, and 11, hence we cannot calculate their importance. To check for these unwanted radical–radical reactions the transient absorbance at 250 nm was measured in experiments using $[\text{CH}_2\text{ClCH}_2\text{Cl}] = 5$ mbar, $[\text{O}_2] = 30$ mbar, and $[\text{SF}_6] = 965$ mbar with the radiolysis dose varied over an order of magnitude. The UV pathlength was 80 cm. Figure 4 shows the observed maximum of the transient absorbance of $\text{CH}_2\text{ClCHClO}_2$ radicals at 250 nm as a function of dose. As seen from Figure 4, the maximum absorption observed in experiments using maximum dose was less than that expected on the basis of a linear extrapolation of the data obtained at lower doses. We ascribe this to incomplete conversion of F atoms into $\text{CH}_2\text{ClCHClO}_2$ radicals caused by secondary radical–radical reactions 8, 10, and 11 at high initial F atoms concentrations.

The solid line drawn through the data in Figure 4 is a linear least-squares fit of the low-dose data. The slope is 0.347 ± 0.027 . From this value and three additional pieces of information, (i) the yield of F atoms of $(3.0 \pm 0.3) \times 10^{15}$ molecule cm^{-3} (full dose and $[\text{SF}_6] = 1000$ mbar), (ii) the conversion of F atoms into $\text{CH}_2\text{ClCHClO}_2$ radicals (95.5%) and FO_2 (4.5%), and (iii) the absorption cross section for FO_2 at 250 nm ($\sigma = 1.3 \times 10^{-18}$ cm^2 molecule $^{-1}$),¹² we derive $\sigma(\text{CH}_2\text{ClCHClO}_2)$ at 250 nm = $(3.53 \pm 0.45) \times 10^{-18}$ cm^2 molecule $^{-1}$. The quoted error includes both statistical and potential systematic errors and so reflects the accuracy of the measurement.

To map out the spectrum of the $\text{CH}_2\text{ClCHClO}_2$ radical, experiments were performed to measure the initial absorbance between 220–300 nm following the pulsed irradiation of $\text{SF}_6/\text{CH}_2\text{ClCH}_2\text{Cl}/\text{O}_2$ mixtures. The initial absorbances were scaled to that at 250 nm and corrected for FO_2 to obtain absolute absorption cross sections. Absorption cross sections are given in Table 1 and compared to the spectrum of CH_2ClO_2 ¹³ in Figure 5. As expected, the $\text{CH}_2\text{ClCHClO}_2$ spectrum is very similar to that of CH_2ClO_2 .

3.5. Kinetic Study of the Self-Reaction of CH_2ClCHCl Radicals. Figure 1A shows a typical absorption trace obtained for the self-reaction of CH_2ClCHCl radicals, together with a nonlinear least-squares second-order decay fit. As discussed in previous publications,^{14,15} the kinetic analysis of second-order decays can be complicated by the formation of products which absorb at the monitoring wavelength. This leads to a positive absorbance after all reactions have ceased. Accordingly, the experimental data were fit with a three parameter expression

$$1/B - 1/B_0 = \ln(10)(2kt)/\sigma_{\text{eff}}L \quad (1)$$

where $B = \log(I_\infty/I)$, $B_0 = \log(I_\infty/I')$, where I' is the minimum transmitted light intensity following the radiolysis pulse, I_∞ is the final light intensity, and I is the transmitted light at time t . k is the second-order rate constant for the self-reaction of the radicals, σ_{eff} is the absorption cross section of the radical minus that of any absorbing product formed at the monitoring wavelength, and L is the monitoring UV path length (80 cm).

The decay of the transient absorption following radiolysis of $\text{CH}_2\text{ClCH}_2\text{Cl}/\text{SF}_6$ mixtures was monitored at a wavelength of 250 nm. The decay was well represented by this second-order least-squares fit. Figure 6 shows the reciprocal half-life for the decay of the absorption at 250 nm as a function of the initial absorbance due to CH_2ClCHCl radicals. A linear least-squares fit of the data in Figure 6 gives a slope of $(6.9 \pm 0.5) \times 10^5$ $\text{s}^{-1} = (k_4 \times 2 \ln 10)/[\sigma(\text{CH}_2\text{ClCHCl})L]$. The intercept of the

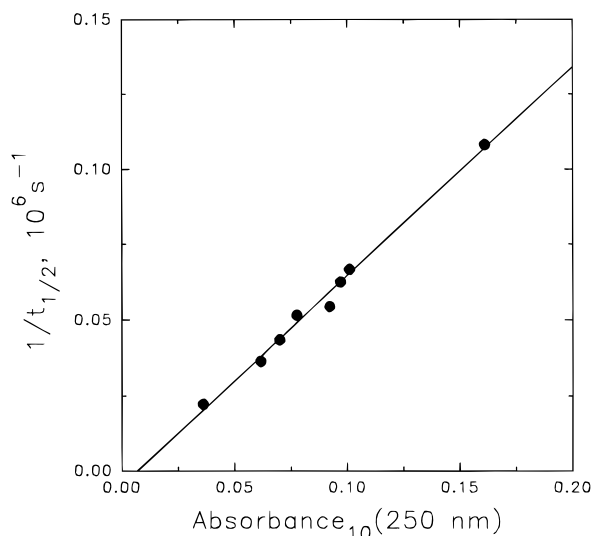


Figure 6. Plot of the reciprocal half-life for the self-reaction of CH_2ClCHCl radicals as a function of the maximum transient absorption at 250 nm.

linear regression of the data is $-(4.8 \pm 5.0) \times 10^3$ s^{-1} and is not significant. Using $\sigma(\text{CH}_2\text{ClCHCl}) = (1.7 \pm 0.2) \times 10^{-18}$ cm^2 molecule $^{-1}$ at 250 nm and the slope $(6.9 \pm 0.5) \times 10^5$ s^{-1} , gives $k_4 = (2.0 \pm 0.3) \times 10^{-11}$ cm^3 molecule $^{-1}$ s^{-1} . This result can be compared to other chloroalkyl radical self-reaction rate constants which range from 2.8×10^{-11} cm^3 molecule $^{-1}$ s^{-1} in the case of CH_2Cl ¹⁶ to 2.4×10^{-12} for CF_3CCl_2 ¹⁷ and follow the sequence CH_2Cl (2.8×10^{-11}) > CH_2ClCHCl (2.0×10^{-11}) > CHCl_2 (9.3×10^{-12})¹⁶ > CCl_3 (4.6×10^{-12})^{18,19} > CF_3CCl_2 (2.4×10^{-12}). This order of reactivity can be rationalized in simple terms on the basis of steric arguments with bulky substituents slowing down the association reaction.

3.6. Kinetic Data for the Reaction $\text{CH}_2\text{ClCHClO}_2 + \text{NO} \rightarrow \text{Products}$. The kinetics of reaction 5 were studied by monitoring the increase in the absorbance at 400 nm, attributed to the formation of NO_2 , following the pulsed radiolysis (53% of maximum dose) of $\text{SF}_6/\text{CH}_2\text{ClCH}_2\text{Cl}/\text{O}_2/\text{NO}$ mixtures. The mixtures were combinations of $[\text{NO}] = 0.23$ – 1.57 mbar, $[\text{CH}_2\text{ClCH}_2\text{Cl}] = 5$ mbar, $[\text{O}_2] = 30$ mbar, and $[\text{SF}_6] = 970$ mbar. This method of determining rate constants of reactions of peroxy radicals with NO has been used extensively in our laboratory and is discussed in detail elsewhere.^{20,21} The absorption transients were fitted using the expression:

$$A(t) = (A_\infty - A_0)[1 - \exp(-k^{\text{1st}}t)] + A_0 \quad (II)$$

where $A(t)$ is the absorbance as a function of time, A_∞ is the absorbance at infinite time, k^{1st} is the pseudo-first-order appearance rate of NO_2 , and A_0 is the extrapolated absorbance at $t = 0$. In the presence of 5 mbar of $\text{CH}_2\text{ClCH}_2\text{Cl}$, F atoms have a lifetime of 0.3 μs with respect to reaction to give CH_2ClCHCl radicals. In the presence of 30 mbar of O_2 , CH_2ClCHCl radicals have a lifetime of 0.5 μs with respect to reaction to give $\text{CH}_2\text{ClCHClO}_2$ radicals. To allow sufficient time for conversion of F atoms into $\text{CH}_2\text{ClCHClO}_2$ radicals the fits were started 2 μs after the radiolysis pulse. In all cases, the rise in absorbance was well fit by first-order kinetics.

Figure 7A shows a plot of the observed pseudo-first-order rate constants, k^{1st} , as a function of $[\text{NO}]$. The initial F atom concentration employed in the present experiments (1.5×10^{15} molecule cm^{-3}) is a significant fraction (4–27%) of that of the initial NO concentration and deviations from pseudo-first-order kinetics may be expected. However, no such deviations were discernable within the experimental data scatter. Assuming that

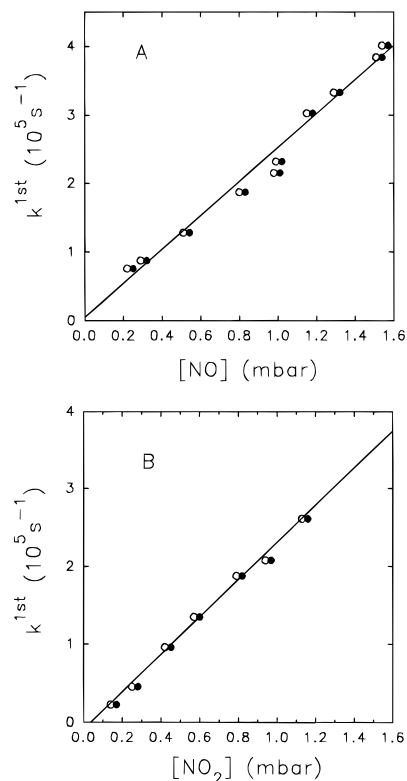


Figure 7. Plot of the pseudo-first-order rate constant for (A) the formation of NO_2 as a function of the NO concentration and for (B) the decay of NO_2 as a function of the NO_2 concentration. Filled symbols are the observed data; open symbols have been corrected by subtracting $[\text{F}]_0/2$. The lines are fits to the corrected data.

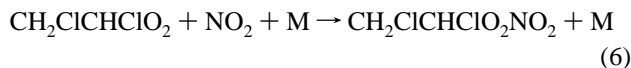
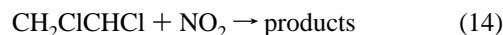
all F atoms either react directly with NO , or produce species that react with NO , then the average NO concentration in a given experiment is less than the initial concentration by an amount equal to $[\text{F}]_0/2$. The open symbols in Figure 7A show the effect of correcting the $[\text{NO}]$ values by this amount. Linear least-squares analysis of the corrected data gives $k_5 = (1.0 \pm 0.1) \times 10^{-11} \text{ cm}^3 \text{ molecule}^{-1} \text{ s}^{-1}$. F atoms also react with NO producing FNO , $k_{12} = 5.5 \times 10^{-12} \text{ cm}^3 \text{ molecule}^{-1} \text{ s}^{-1}$.²² FNO does not absorb at 400 nm ²³ and reaction 12 has no influence on the kinetic analysis used to derive k_5 .



The reaction of $\text{CH}_2\text{ClCHClO}_2$ radicals with NO produces NO_2 and, by inference, $\text{CH}_2\text{ClCHClO}$ radicals. The alkoxy radical $\text{CH}_2\text{ClCHClO}$ can react with O_2 , or decompose. If reaction with O_2 or decomposition occurs within the time scale of the present experiments ($0\text{--}10 \mu\text{s}$) new peroxy radicals will be formed which can undergo subsequent reaction with NO to give more NO_2 . In the present experiments the yield of NO_2 , calculated using $\sigma_{\text{NO}_2}(400 \text{ nm}) = 6 \times 10^{-19} \text{ cm}^2 \text{ molecule}^{-1}$,²⁴ was $162 \pm 17\%$. Corrections were made for the consumption of F atoms by reaction with O_2 and NO . The fact that the NO_2 yield is greater than 100% shows that $\text{CH}_2\text{ClCHClO}$ radicals either react with O_2 , or decompose, within the experimental timescale of $0\text{--}10 \mu\text{s}$. Because of the formation of NO_2 from reactions occurring subsequent to reaction 5 the rate constant $k_5 = (1.0 \pm 0.1) \times 10^{-11} \text{ cm}^3 \text{ molecule}^{-1} \text{ s}^{-1}$ determined in the present work should be regarded as a lower limit for the rate constant for reaction 5. Hence, $k_5 > 9 \times 10^{-12} \text{ cm}^3 \text{ molecule}^{-1} \text{ s}^{-1}$. This value is consistent with rate constants determined previously for reactions of other peroxy radicals with NO .²¹

In section 3.9 we show that for the experimental conditions of the above experiments (30 mbar of O_2) 98% of the $\text{CH}_2\text{ClCHClO}$ radicals will undergo decomposition while 2% will react with O_2 . The fact that the NO_2 yield is substantially greater than 100% is therefore due to the rapid decomposition of $\text{CH}_2\text{ClCHClO}$ radicals. In all experiments the rise in the transient absorption at 400 nm followed first-order kinetics. It follows that the rate of decomposition of $\text{CH}_2\text{ClCHClO}$ radicals must be faster than the fastest pseudo-first-order rate measured, i.e., $> 4 \times 10^5 \text{ s}^{-1}$.

3.7. Kinetic Data of the Reaction $\text{CH}_2\text{ClCHClO}_2 + \text{NO}_2 + \text{M} \rightarrow \text{CH}_2\text{ClCHClO}_2\text{NO}_2 + \text{M}$. The kinetics of reaction 6 were studied by monitoring the decrease in absorbance at 400 nm following the pulsed radiolysis (53% of maximum dose) of mixtures of 5 mbar of $\text{CH}_2\text{ClCH}_2\text{Cl}$, 30 mbar of O_2 , 0.28–1.16 mbar NO_2 , and SF_6 to 1000 mbar total pressure. This method of measuring rate constants of reactions of peroxy radicals with NO_2 has been used extensively in our laboratory and is discussed elsewhere.²⁵ The rate of decay of the absorbance at 400 nm followed first-order kinetics and increased with increasing NO_2 concentration. It seems reasonable to explain the loss in absorbance by a loss of NO_2 . Three reactions could be responsible:



Under the present experimental conditions with $[\text{CH}_2\text{ClCH}_2\text{Cl}] = 5 \text{ mbar}$ and $[\text{O}_2] = 30 \text{ mbar}$, reactions 13 and 14 will be of negligible importance.

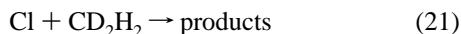
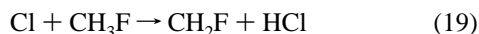
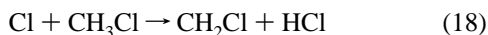
Values of the observed pseudo-first-order rate constants of NO_2 loss derived by fitting a first-order decay to the observed transients are plotted as a function of $[\text{NO}_2]$ in Figure 7B. The initial F atom concentration employed in the present experiments ($1.5 \times 10^{15} \text{ molecule cm}^{-3}$) is a significant fraction (5–22%) of that of the initial NO_2 concentration and deviations from pseudo-first-order kinetics may be expected. However, no such deviations were discernable within the experimental data scatter. Assuming that all F atoms either react directly with NO_2 or produce species that react with NO_2 then the average NO_2 concentration in a given experiment is less than the initial concentration by an amount equal to $[\text{F}]_0/2$. The open symbols in Figure 7B show the effect of this correction. Corrections applied were in the range 3–11%. Linear least-squares analysis of the corrected data gives $k_6 = (9.8 \pm 0.6) \times 10^{-12} \text{ cm}^3 \text{ molecule}^{-1} \text{ s}^{-1}$.

The reactions of peroxy radicals with NO_2 are pressure dependent and are generally at, or near, the high pressure limit at 1 atmosphere total pressure of SF_6 diluent.¹⁰ The value of k_6 measured here is entirely consistent with the high-pressure limiting rate constants previously determined for such reactions which typically lie in the range $(5\text{--}10) \times 10^{-12} \text{ cm}^3 \text{ molecule}^{-1} \text{ s}^{-1}$.¹⁰

3.8. Kinetics of the Reactions of Cl Atoms with $\text{CH}_2\text{ClCH}_2\text{Cl}$ and $\text{CH}_2\text{ClC}(\text{O})\text{Cl}$. Prior to investigating the atmospheric fate of $\text{CH}_2\text{ClCHClO}$ radicals, a series of relative rate experiments was performed using the FTIR system to investigate the kinetics of the reactions of Cl atoms with $\text{CH}_2\text{ClCH}_2\text{Cl}$ and $\text{CH}_2\text{ClC}(\text{O})\text{Cl}$. The techniques used are described in detail elsewhere.²⁶ Photolysis of molecular chlorine was used as a source of Cl atoms.



The kinetics of reaction 16 were measured relative to reactions 18 and 19, reaction 17 was studied relative to reactions 20–22.

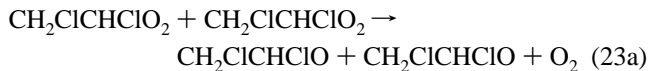


The observed losses of $\text{CH}_2\text{ClCH}_2\text{Cl}$ vs CH_3Cl and CH_3F , and $\text{CH}_2\text{ClC(O)Cl}$ vs CD_4 , CD_2H_2 , and CH_4 following the UV irradiation of $\text{CH}_2\text{ClCH}_2\text{Cl}/\text{CH}_3\text{Cl}/\text{Cl}_2$, $\text{CH}_2\text{ClCH}_2\text{Cl}/\text{CH}_3\text{F}/\text{Cl}_2$, and $\text{CH}_2\text{ClC(O)Cl}/\text{methane}/\text{Cl}_2$ mixtures, in 700 Torr total pressure of N_2 , or air, diluent are shown in Figures 8 and 9. There was no discernable difference between data obtained in N_2 or air. Linear least-squares analysis gives $k_{16}/k_{18} = 2.65 \pm 0.18$, $k_{16}/k_{19} = 3.90 \pm 0.12$, $k_{17}/k_{20} = 11.1 \pm 1.5$, $k_{17}/k_{21} = 1.40 \pm 0.07$, and $k_{17}/k_{22} = 0.61 \pm 0.04$. Using $k_{18} = 4.9 \times 10^{-13,24}$, $k_{19} = 3.2 \times 10^{-13,27}$, $k_{20} = 6.1 \times 10^{-15,26}$, $k_{21} = 4.5 \times 10^{-14,26}$ and $k_{22} = 1.0 \times 10^{-13,24}$ gives $k_{16} = (1.30 \pm 0.09) \times 10^{-12}$, $k_{16} = (1.25 \pm 0.10) \times 10^{-12}$, $k_{17} = (6.8 \pm 0.9) \times 10^{-14}$, $k_{17} = (6.3 \pm 0.3) \times 10^{-14}$, and $k_{17} = (6.1 \pm 0.4) \times 10^{-14} \text{ cm}^3 \text{ molecule}^{-1} \text{ s}^{-1}$, respectively. Consistent results were obtained using the different reference compounds. We choose to quote values for k_{16} and k_{17} which are averages of the results above with error limits which encompass the extremes of the ranges, hence $k_{16} = (1.28 \pm 0.13) \times 10^{-12}$ and $k_{17} = (6.4 \pm 1.3) \times 10^{-14} \text{ cm}^3 \text{ molecule}^{-1} \text{ s}^{-1}$. We estimate that potential systematic errors associated with uncertainties in the reference rate constants could add an additional 10% to the uncertainty range. Propagating this additional 10% uncertainty gives $k_{16} = (1.3 \pm 0.2) \times 10^{-12}$ and $k_{17} = (6.4 \pm 1.4) \times 10^{-14} \text{ cm}^3 \text{ molecule}^{-1} \text{ s}^{-1}$.

The kinetics of reaction 16 have been studied previously by Wine and Semmes²⁸ and Tschuikow-Roux et al.²⁹ Using an absolute rate technique, Wine et al.²⁸ measured $k_{16} = 1.5 \times 10^{-12}$ at room temperature while Tschuikow-Roux et al.²⁹ used a relative rate method to derive $k_{12} = 1.3 \times 10^{-12} \text{ cm}^3 \text{ molecule}^{-1} \text{ s}^{-1}$. The value of k_{16} measured in the present work is consistent with both previous determinations. There are no literature data for k_{17} to compare with our result.

3.9. Study of the Atmospheric Fate of $\text{CH}_2\text{ClCHClO}$ Radicals. To determine the atmospheric fate of the alkoxy radical $\text{CH}_2\text{ClCHClO}$, experiments were performed in which $\text{Cl}_2/\text{CH}_2\text{ClCH}_2\text{Cl}/\text{O}_2$ mixtures at a total pressure of 700 Torr (N_2 diluent) were irradiated in the FTIR–smog chamber system. The loss of $\text{CH}_2\text{ClCH}_2\text{Cl}$ and the formation of products were monitored by FTIR spectroscopy. By analogy to the behavior of other peroxy radicals^{9,10} it is expected that $\text{CH}_2\text{ClCHClO}$

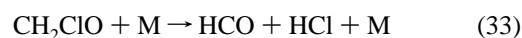
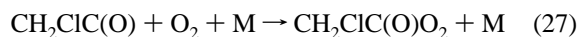
radicals will be formed in the chamber by the self-reaction of $\text{CH}_2\text{ClCHClO}_2$ radicals.



The alkoxy radical will then either react with O_2 , decompose via intramolecular HCl elimination, or undergo C–C bond scission:



The subsequent reactions of the radical species formed in reactions 25 and 26 will include:



The goal of the FTIR experiments was to determine the relative importance of reactions 24–26 in the atmospheric chemistry of $\text{CH}_2\text{ClCHClO}$ radicals. $\text{CH}_2\text{ClC(O)Cl}$ product serves as a marker for reaction 24. Reaction 25 will lead to an observed HCl yield (defined as moles of HCl formed per mole of $\text{CH}_2\text{ClCH}_2\text{Cl}$ lost) which is in excess of 100% and to substantial CO_2 and HC(O)Cl product formation. If reaction 26 is important then high yields of HC(O)Cl are expected with no CO_2 and no excess HCl.

In the Cl atom-initiated oxidation of $\text{CH}_2\text{ClCH}_2\text{Cl}$, three carbon-containing products were readily identified by virtue of their characteristic IR features: CO_2 , HC(O)Cl , and $\text{CH}_2\text{ClC(O)Cl}$. The yields of these species following the UV irradiation of a mixture of 275 mTorr of $\text{CH}_2\text{ClCH}_2\text{Cl}$ and 147 mTorr of Cl_2 in 700 Torr total pressure of air are shown as a function of the $\text{CH}_2\text{ClCH}_2\text{Cl}$ loss in Figure 10. As seen from Figure 10, the formation of HCl, CO_2 , HC(O)Cl , and $\text{CH}_2\text{ClC(O)Cl}$ increased linearly with the loss of $\text{CH}_2\text{ClCH}_2\text{Cl}$. Such linear behavior suggests the absence of significant complications caused by secondary reactions in the system. At this point it is germane

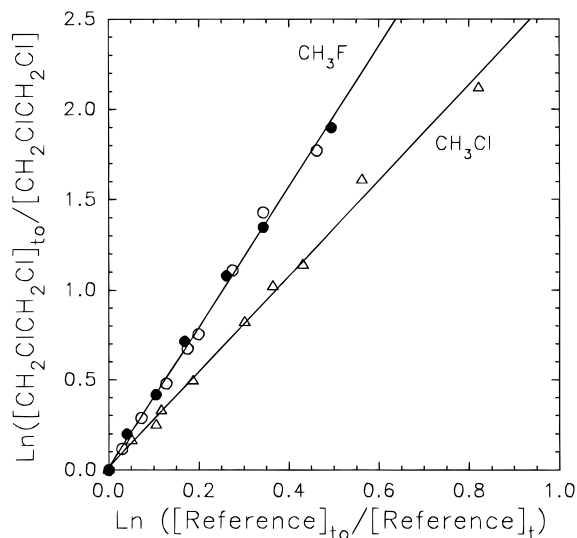


Figure 8. Observed loss of $\text{CH}_2\text{ClCH}_2\text{Cl}$ vs CH_3F (circles) and CH_3Cl (triangles) in the presence of Cl atoms in 700 Torr of either air (filled symbols) or N_2 (open symbols) diluent.

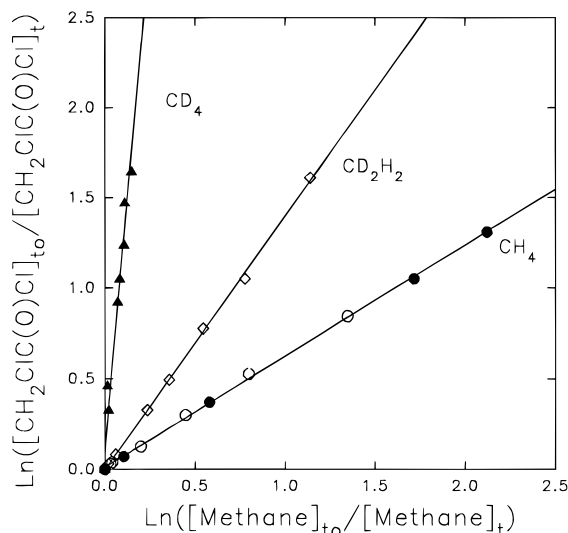


Figure 9. Observed loss of $\text{CH}_2\text{ClC(O)Cl}$ vs CD_4 (triangles), CD_2H_2 (diamonds), and CH_4 (circles) in the presence of Cl atoms in 700 Torr of either air (filled symbols) or N_2 (open symbols) diluent.

to consider possible losses of these products in the chamber. None of the products are expected to be photolyzed by the UV blacklamps used in this work. To check for possible heterogeneous losses, reaction mixtures were allowed to stand in the dark for 20 min; there were no observable losses ($<2\%$) of any of these compounds. There is no reaction of Cl atoms with CO_2 or HCl. $\text{CH}_2\text{ClCH}_2\text{Cl}$ reacts 1.8 ($1.3 \times 10^{-12}/7.3 \times 10^{-13}$ ^{30,31}) and 20 ($1.3 \times 10^{-12}/6.4 \times 10^{-14}$) times more rapidly with Cl atoms than HC(O)Cl and $\text{CH}_2\text{ClC(O)Cl}$, respectively. Hence, for the consumptions of $\text{CH}_2\text{ClCH}_2\text{Cl}$ employed in the present work ($<11\%$) loss of HC(O)Cl and $\text{CH}_2\text{ClC(O)Cl}$ via Cl atom attack is of minor importance.

The observation of CO_2 as a primary product following Cl atom attack of $\text{CH}_2\text{ClCH}_2\text{Cl}$ in air is interesting as such formation of CO_2 requires a rather dramatic change in molecular configuration with the breakage of a C–C bond, C–Cl bond, and two C–H bonds and the formation of two C=O bonds. To check for a contribution of secondary reactions involving Cl atoms to the observed CO_2 yield requires experiments to be performed in which the consumption of $\text{CH}_2\text{ClCH}_2\text{Cl}$ is less than 1%. Such a small consumption cannot be measured directly. However, it can be measured indirectly using experi-

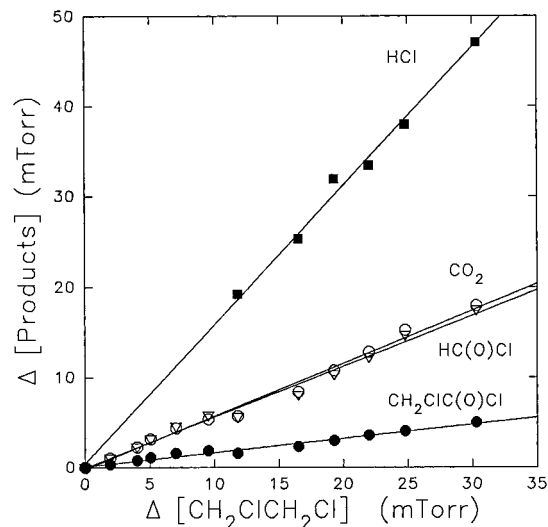


Figure 10. Yields of HCl (■), CO_2 (○), HC(O)Cl (▽), and $\text{CH}_2\text{ClC(O)Cl}$ (●) vs the $\text{CH}_2\text{ClCH}_2\text{Cl}$ loss observed following the UV irradiation of $\text{CH}_2\text{ClCH}_2\text{Cl}/\text{Cl}_2$ mixtures in 700 Torr of air diluent at 296 K. The $\text{CH}_2\text{ClCH}_2\text{Cl}$ loss was observed directly for $\Delta[\text{CH}_2\text{ClCH}_2\text{Cl}] > 10$ mTorr. Losses of $\text{CH}_2\text{ClCH}_2\text{Cl} < 10$ mTorr were calculated from the observed loss of CH_3OCH_3 tracer, see text.

ments in which a more reactive species such as CH_3OCH_3 is present as a tracer. Experiments were performed using a mixture of 979 mTorr of $\text{CH}_2\text{ClCH}_2\text{Cl}$, 11.4 mTorr of CH_3OCH_3 , and 147 mTorr of Cl_2 in 700 Torr of air diluent. CH_3OCH_3 reacts with Cl atoms a factor of 146 ($1.9 \times 10^{-10}/1.3 \times 10^{-12}$) times faster than does $\text{CH}_2\text{ClCH}_2\text{Cl}$. The consumption of CH_3OCH_3 was monitored by virtue of its IR features at $1300\text{--}1400\text{ cm}^{-1}$ and used in the expression, $\ln([\text{CH}_3\text{OCH}_3]_{t0}/[\text{CH}_3\text{OCH}_3]_t) = 146 \ln([\text{CH}_2\text{ClCH}_2\text{Cl}]_{t0}/[\text{CH}_2\text{ClCH}_2\text{Cl}]_t)$, to compute the consumption of $\text{CH}_2\text{ClCH}_2\text{Cl}$. The calculated consumption of $\text{CH}_2\text{ClCH}_2\text{Cl}$ was 1.9–9.5 mTorr (0.2–1.0% of the initial concentration). The Cl atom-initiated oxidation of CH_3OCH_3 gives CH_3OCHO and $\text{CH}_3\text{OCH}_2\text{OOH}$ ³² and is not expected to interfere with the oxidation of $\text{CH}_2\text{ClCH}_2\text{Cl}$. The observed yields of CO_2 , HC(O)Cl , and $\text{CH}_2\text{ClC(O)Cl}$ are plotted vs the calculated $\text{CH}_2\text{ClCH}_2\text{Cl}$ loss in Figure 10. For experiments in which CH_3OCH_3 was used as a tracer for the $\text{CH}_2\text{ClCH}_2\text{Cl}$ loss the HCl yield does not provide any useful information and so it is not plotted in Figure 10. As seen from Figure 10, there is good agreement between the data obtained using CH_3OCH_3 as a tracer for $\text{CH}_2\text{ClCH}_2\text{Cl}$ loss and those experiments in which the $\text{CH}_2\text{ClCH}_2\text{Cl}$ loss was observed directly. In the combined data set shown in Figure 10 the $\text{CH}_2\text{ClCH}_2\text{Cl}$ consumption ranged from 0.2–11%. The consistency of the results over this consumption range precludes the possibility that the CO_2 product is formed indirectly by secondary reactions involving Cl atom attack of some unknown reactive intermediate.

The CO_2 , HC(O)Cl , and $\text{CH}_2\text{ClC(O)Cl}$ products shown in Figure 10 together account for $74 \pm 15\%$ of the loss of $\text{CH}_2\text{ClCH}_2\text{Cl}$. In addition to these identified products IR features due to unidentified products were observed at 1052, 1117, 1187, 1362, and 1450 cm^{-1} . As described above there are a variety of different peroxy radicals formed in the present experimental system; $\text{CH}_2\text{ClCHClO}_2$, $\text{CH}_2\text{ClC(O)O}_2$, CH_2ClO_2 , and HO_2 . These species may undergo cross reactions to give a variety of products. The fact that the combined yields of CO_2 , HC(O)Cl , and $\text{CH}_2\text{ClC(O)Cl}$ products only account for 75% of the loss of $\text{CH}_2\text{ClCH}_2\text{Cl}$ is not surprising in light of the complexity of the peroxy radical chemistry.

Linear least-squares analysis of the data in Figure 10 gives yields of $154 \pm 8\%$, $59 \pm 4\%$, $56 \pm 4\%$, and $16 \pm 2\%$ for

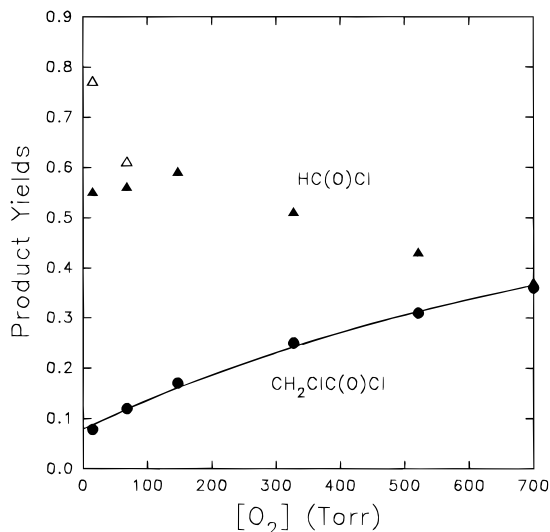


Figure 11. Yields of HC(O)Cl (triangles) and CH₂CIC(O)Cl (circles) vs the O₂ partial pressure following the UV irradiation of CH₂CICH₂Cl/Cl₂/O₂ mixtures in 700 Torr total pressure made up with N₂ diluent at 296 K. Open symbols have been corrected for the effect of reaction 33—see text for details. The curve through the CH₂CIC(O)Cl data is a fit of the expression discussed in the text.

HCl, CO₂, HC(O)Cl, and CH₂CIC(O)Cl, respectively. The observation of a yield of HCl which is greater than 100% together with a substantial CO₂ yield shows that intramolecular elimination of HCl via reaction 25 is an important loss mechanism for CH₂CICHClO radicals in the chamber. This behavior is similar to that displayed by CH₃CHClO radicals which undergo rapid HCl elimination.^{1,2,4} It is interesting to note that the HCl yield in Figure 10 is in excess of the expected 100% yield attributable to reaction 16 by an amount (54 ± 8%) which is indistinguishable from the observed CO₂ and HC(O)Cl yields. In 700 Torr of air diluent each CO₂ molecule formed in reaction 29 will be accompanied by the formation of one molecule of HC(O)Cl via reactions 30–32. The fact that the CO₂ and HC(O)Cl yields shown in Figure 10 are indistinguishable shows that reaction 26 does not play a significant (<10%) role in the chemistry of CH₂CICHClO radicals. The CH₂CIC(O)Cl product shown in Figure 10 can be formed via either the molecular channel of the self-reaction of CH₂CICHClO₂ radicals, reaction 23b, or via reaction of O₂ with the alkoxy radical CH₂CICHClO, reaction 24. If reaction 24 is a substantial source of CH₂CIC(O)Cl then its yield should be sensitive to the partial pressure of O₂.

A series of experiments were performed using mixtures of 120 mTorr of CH₂CICH₂Cl, 34–176 mTorr of Cl₂, 15–700 Torr of O₂, in 700 Torr total pressure of N₂ diluent. Figure 11 shows the yields of HC(O)Cl and CH₂CIC(O)Cl plotted as a function of the O₂ partial pressure. HC(O)Cl is formed by reaction of CH₂ClO radicals with O₂, reaction 32. For the two lowest O₂ partial pressures investigated, CH₂ClO radicals will be lost via both reactions 32 and 33. While for [O₂] > 100 Torr reaction 32 totally dominates reaction 33. To place the observed HC(O)Cl yields on an equal footing, the loss of CH₂ClO radicals via reaction 33 was computed using $k_{32}/k_{33} = 5.0 \times 10^{-18} \text{ cm}^3 \text{ molecule}^{-1}$.³ The observed yields of HC(O)Cl for the experiments using low [O₂] were then corrected upward to give values expected if all CH₂ClO radicals were converted into HC(O)Cl.

As seen from Figure 11, the yield of CH₂CIC(O)Cl increased with increasing O₂ concentration while the HC(O)Cl yield decreased. Assuming that CH₂CIC(O)Cl is formed in the chamber solely by reactions 23b and 24 then its yield can be

expressed as a function of the rate constant ratio k_{24}/k_{25} and the CH₂CIC(O)Cl yield from reaction 23b, Y_o .³³

CH₂CIC(O)Cl yield =

$$Y_o + (1 - 2Y_o) \left(\frac{(k_{24}/k_{25})[O_2]}{1 + (k_{24}/k_{25})[O_2]} \right)$$

The solid line in Figure 11 is a fit of the above expression to the data which gives $k_{24}/k_{25} = (2.3 \pm 0.2) \times 10^{-20} \text{ cm}^3 \text{ molecule}^{-1}$ and $Y_o = 0.08 \pm 0.02$. From this rate constant ratio it can be calculated that in one atmosphere of air at 296 K, 89% of the CH₂CICHClO radicals decompose via HCl elimination while 11% react with O₂. Intramolecular elimination of HCl dominates the fate of CH₂CICHClO radicals at sea level. With increasing altitude in the atmosphere the temperature, total pressure, and partial pressure of O₂ all decrease. Decreasing temperature and total pressure favor reaction 24 over reaction 25 while decreasing partial pressure of O₂ will favor reaction 25 over reaction 24. Reaction 25 is a unimolecular decomposition reaction and is expected to be very sensitive to changes in temperature. Considering the conditions pertinent to the United States standard atmosphere over the altitude range 0–15 km³⁴ and neglecting the effect of total pressure, reaction 25 will slow down faster than reaction 24 if the activation energy for reaction 25 is > 4 kcal mol⁻¹ more than that for reaction 24. By analogy to the behavior of CH₂ClO radicals⁶ it seems likely that the barrier to decomposition of CH₂CICHClO radicals will be more than 4 kcal mol⁻¹ larger than that for reaction with O₂. Hence, it is expected that reaction with O₂ will increase in importance with increasing altitude. In the absence of data concerning the temperature dependence of the rate constant ratio k_{24}/k_{25} we are unable to provide an overall assessment of the relative importance of reactions 24 and 25 in the atmospheric chemistry of CH₂CICHClO radicals.

Finally, it is of interest to compare the behavior of CH₂CICHClO radicals observed here with that reported for CH₂FCHFO radicals.³⁵ We show here that CH₂CICHClO radicals undergo 3-center intramolecular HCl elimination. No such analogous process is observed for CH₂FCHFO radicals which undergo C–C bond scission exclusively under ambient conditions.

3.10. The Mechanism of the Reaction of F Atoms with CH₂CICH₂Cl. As discussed in section 3.1, we assume that reaction of F atoms with CH₂CICH₂Cl proceeds exclusively via H atom abstraction. For completeness, the FTIR system was used to study the F atom initiated oxidation of CH₂CICH₂Cl. HC(O)Cl and CH₂CIC(O)Cl were observed in yields of 39 ± 2% and 38 ± 2% following the irradiation of a mixture of 121 mTorr of CH₂CICH₂Cl and 444 mTorr of F₂ in 700 Torr of O₂. These yields are indistinguishable from those observed in Cl atom initiated experiments (see Figure 11) providing experimental support for the expectation that reaction of F atoms with CH₂CICH₂Cl gives CH₂CICHCl radicals.

4. Implications for Atmospheric Chemistry

Following release into the atmosphere, CH₂CICH₂Cl will react predominantly with hydroxyl radicals. At 298 K the rate constant for reaction of OH radicals with CH₂CICH₂Cl is 25 (2.4 × 10⁻¹³–9.6 × 10⁻¹⁵)^{36,37} times greater than that of methyl chloroform which is known to be removed from the atmosphere solely by reaction with OH radicals with an atmospheric lifetime of 5.7 years.³⁷ Hence, the atmospheric lifetime of CH₂CICH₂Cl is ~3 months. Reaction with OH gives CH₂CICHCl radicals. Using $k_2 = 3.0 \times 10^{-12} \text{ cm}^3 \text{ molecule}^{-1} \text{ s}^{-1}$, it can be calculated that in 760 Torr of air, CH₂CICHCl radicals have a lifetime of 0.06 μs with respect to reaction with O₂ to give peroxy radicals,

CH₂ClCHClO₂. CH₂ClCHClO₂ radicals react rapidly with NO to produce NO₂ and (by inference) CH₂ClCHClO radicals. Using $k_5 \geq 9.0 \times 10^{-12} \text{ cm}^3 \text{ molecule}^{-1} \text{ s}^{-1}$ together with an estimated background tropospheric NO concentration of $2.5 \times 10^8 \text{ cm}^{-3}$ ³⁸ the lifetime of CH₂ClCHClO₂ radicals with respect to reaction 5 is calculated to be less than 7 min. Reaction 5 is likely to be an important atmospheric loss of CH₂ClCHClO₂ radicals. Reaction with O₂ and intramolecular HCl elimination are competing atmospheric fates of CH₂ClCHClO radicals. In one atmosphere of air at 296 K, 89% of the CH₂ClCHClO radicals decompose via HCl elimination while 11% react with O₂. Reaction with O₂ gives CH₂ClC(O)Cl while HCl elimination leads to the formation of HC(O)Cl. Both compounds have lifetimes in the lower atmosphere which are much shorter than that required for transport to the stratosphere and so are incapable of delivering significant amounts of chlorine to the stratosphere.

We show here that CH₂ClCHClO radicals undergo rapid ($k_{25} > 4 \times 10^5 \text{ s}^{-1}$) intramolecular HCl elimination. This behavior has also been reported from the structurally similar CH₂ClO and CH₃CHClO radicals.¹⁻⁶ It appears that intramolecular HCl elimination is a general mechanism for α -monochloroalkoxy radical loss which should be considered in future assessments of the atmospheric chemistry of chlorinated organic compounds.

Acknowledgment. We thank Steve Japar (Ford Motor Company) for a critical reading of the manuscript and Marchoe Dill for technical assistance.

References and Notes

- (1) Shi, J.; Wallington, T. J.; Kaiser, E. W. *J. Phys. Chem.* **1993**, *97*, 6184.
- (2) Maricq, M. M.; Shi, J.; Szente, J. J.; Rimai, L.; Kaiser, E. W. *J. Phys. Chem.* **1993**, *97*, 9686.
- (3) Kaiser, E. W.; Wallington, T. J. *J. Phys. Chem.* **1994**, *98*, 5679.
- (4) Kaiser, E. W.; Wallington, T. J. *J. Phys. Chem.* **1995**, *99*, 8669.
- (5) Nielsen, O. J. Risø Report R-480, 1984.
- (6) Wallington, T. J.; Orlando, J. J.; Tyndall, G. S. *J. Phys. Chem.* **1995**, *99*, 9437.
- (7) Stein, S. E.; Rukkens, J. M.; Brown, R. L. NIST Structures and Properties Database Ver. 1.2; NIST: Gaithersburg, MD, 1991.
- (8) Rasmussen, O. L.; Bjergbakke, E. B. Risø Report R-395, 1984.
- (9) Wallington, T. J.; Dagaut, P.; Kurylo, M. J. *Chem. Rev.* **1992**, *92*, 667.
- (10) Lightfoot, P. D.; Cox, R. A.; Crowley, J. N.; Destriau, M.; Hayman, G. D.; Jenkin, M. E.; Moortgat, G. K.; Zabel, F. *Atmos. Environ.* **1992**, *26A*, 1805.

- (11) Wallington, T. J.; Ellermann, T.; Nielsen, O. J. *J. Phys. Chem.* **1993**, *97*, 8442.
- (12) Ellermann, T.; Sehested, J.; Nielsen, O. J.; Pagsberg, P.; Wallington, T. J. *Chem. Phys. Lett.* **1993**, *218*, 287.
- (13) Dagaut, P.; Wallington, T. J.; Kurylo, M. J. *Int. J. Chem. Kinet.* **1988**, *20*, 815.
- (14) Kurylo, M. J.; Ouellette, P. A.; Laufer, A. H. *J. Phys. Chem.* **1986**, *90*, 437.
- (15) Sander, S. P.; Watson, R. T. *J. Phys. Chem.* **1981**, *86*, 2960.
- (16) Roussel, P. B.; Lightfoot, P. D.; Caralp, F.; Catoire, V.; Lesclaux, R.; Forst, W. *J. Chem. Soc., Faraday Trans.* **1991**, *87*, 2367.
- (17) Wallington, T. J.; Ellermann, T.; Nielsen, O. J. *Res. Chem. Intermed.* **1994**, *20*, 265.
- (18) Danis, F.; Caralp, F.; Veyret, B.; Loirat, H.; Lesclaux, R. *Int. J. Chem. Kinet.* **1989**, *21*, 715.
- (19) Ellermann, T. *Chem. Phys. Lett.* **1992**, *189*, 175.
- (20) Wallington, T. J.; Nielsen, O. J. *Chem. Phys. Lett.* **1991**, *187*, 33.
- (21) Sehested, J.; Nielsen, O. J.; Wallington, T. J. *Chem. Phys. Lett.* **1993**, *213*, 457.
- (22) Wallington, T. J.; Ellermann, T.; Nielsen, O. J.; Sehested, J. *J. Phys. Chem.* **1994**, *98*, 2346.
- (23) Sehested, J.; Nielsen, O. J. *Chem. Phys. Lett.* **1993**, *206*, 369.
- (24) DeMore, W. B.; Sander, S. P.; Golden, D. M.; Hampson, R. F.; Kurylo, M. J.; Howard, C. J.; Ravishankara, A. R.; Kolb, C. E.; Molina, M. J. *Jet Propulsion Laboratory Publication 94-26*; Jet Propulsion Laboratory: Pasadena, CA, 1994.
- (25) Platz, J.; Nielsen, O. J.; Sehested, J.; Wallington, T. J. *J. Phys. Chem.* **1995**, *99*, 6570.
- (26) Wallington, T. J.; Hurley, M. D. *Chem. Phys. Lett.* **1992**, *189*, 437.
- (27) Wallington, T. J.; Ball, J. C.; Nielsen, O. J.; Bartkiewicz, E. *J. Phys. Chem.* **1992**, *96*, 1241.
- (28) Wine, P. H.; Semmes, D. M. *J. Phys. Chem.* **1983**, *87*, 3572.
- (29) Tschuikow-Roux, E.; Faraji, F.; Niedzielski, J. *Int. J. Chem. Kinet.* **1986**, *18*, 513.
- (30) Niki, H.; Maker, P. D.; Savage, C. M.; Breitenbach, L. P. *Int. J. Chem. Kinet.* **1980**, *12*, 915.
- (31) Libuda, H. G.; Zabel, F.; Fink, E. H.; Becker, K. H. *J. Phys. Chem.* **1990**, *94*, 5860.
- (32) Jenkin, M. E.; Hayman, G. D.; Wallington, T. J.; Hurley, M. D.; Nielsen, O. J.; Ellermann, T. *J. Phys. Chem.* **1993**, *97*, 11712.
- (33) Wallington, T. J.; Hurley, M. D.; Ball, J. C.; Kaiser, E. W. *Environ. Sci. Technol.* **1992**, *26*, 1318.
- (34) *U.S. Standard Atmosphere, 1976*; NOAA, NASA, USAF: Washington, DC, 1976.
- (35) Wallington, T. J.; Hurley, M. D.; Ball, J. C.; Ellermann, T.; Nielsen, O. J.; Sehested, J. *J. Phys. Chem.* **1994**, *98*, 5435.
- (36) Mallard, W. G.; Westley, F.; Hampson, R. F.; Frizzell, D. H. *NIST Chemical Kinetics Database, Ver. 5.0*; NIST: Gaithersburg, MD, 1993.
- (37) Ravishankara, A. R.; Lovejoy, E. R. *J. Chem. Soc., Faraday Trans.* **1994**, *90*, 2159.
- (38) Atkinson, R. World Meteorological Organization Global Ozone Research and Monitoring Project, Report No. 20; Scientific Assessment of Stratospheric Ozone, 1989; Vol. 2, p 167.

JP952149G